The counterintuitive mechanical response in simple tension of arterial models that are separable functions of the I_1, I_4, I_6 invariants

J.G. Murphy[a,b,*], S. Biwa[c]

[a]Department of Mechanical Engineering,
Dublin City University, Glasnevin, Dublin 9, Ireland;

[b]School of Mathematics, Statistics and Applied Mathematics,
National University of Ireland Galway, Ireland;

[c]Department of Aeronautics and Astronautics,
Kyoto University, Katsura, Nishikyo-ku 615-8540, Japan.

[*]corresponding author   email: jeremiah.murphy@dcu.ie, phone: +353-1-700-8924

Abstract

It is shown that some of the orthotropic models reported in the literature for the mechanical response of elastic arteries and which assume a separable dependence on the I_1, I_4, I_6 invariants predict curious and unexpected behaviour in simple tension. Specifically it is shown that the out-of-plane stress response can be stiffer than the in-plane over a moderate range of strain and that when the in-plane response is much stiffer than the out-of-plane, as might be expected for a fibre-reinforced material, it is accompanied by a large auxetic response in the out-of-plane direction. This mechanical response for this class of orthotropic materials seems counterintuitive and it is hypothesised that it could be due to their well-known inability to fully recover the linear theory, on restriction to infinitesimal deformations. A generalisation of these models that is fully compatible with the linear theory is proposed. An alternative strategy of assuming that the fibres cannot support compression is shown not to be a universal remedy.

1 Introduction

The phenomenological theory of non-linear, incompressible elasticity proposed by Rivlin (1948) has been extensively employed in predicting the mechanical response of biological, soft tissue. The degree of anisotropy used in the modelling process is typically motivated by the morphology of the tissue under consideration. A balance has to be struck between simplicity of form of the mathematical model so that predictions can be efficiently made and the necessarily complex structure of the biological tissue. One influential illustration

of this is the model of Holzapfel *et al.* (2000) who proposed that elastic arteries could be modelled as a non-linear, isotropic matrix in which are embedded two helically wound families of mechanically equivalent fibres. Unfortunately, even with this idealisation, the corresponding mathematical model poses formidable technical challenges, prompting further simplifying constitutive assumptions to be made by Holzapfel *et al.* (2000). It is the effect of these assumptions on the predictive capability of the model that is of interest here.

Simplifying assumptions in the theory of non-linear elasticity in order to reduce its technical complexity have a long history, going back to Rivlin himself. While there has always been the realisation that simplifying assumptions must necessarily compromise the accuracy of model predictions, attention has been drawn recently to the shortcomings of some of the reduced models for the mechanical response of arteries. If the reduced models are assumed dependent solely on the I_1, I_4, I_6 invariants, using the standard notation for the strain invariants for orthotropic materials, Murphy (2014) has shown that the corresponding linear theory cannot be fully recovered on restriction to infinitesimal deformations, a necessary condition for non-linear models. Horgan and Murphy (2014) have also shown that these anisotropic materials behave as if they were isotropic for two important modes of inhomogeneous shearing for cylindrical vessels, indicating possible deficiencies in shear stress predictions. Despite these drawbacks, these models have become the *de facto* standard for modelling the mechanical response of elastic arteries and are implemented in many commercial Finite Element codes.

Some further idiosyncrasies of these models are highlighted here. Simple tension experiments are central to the identification of material parameters for many models of the mechanical response of soft tissue and are considered here for orthotropic materials with two families of straight, mechanically equivalent fibres parallel to two opposite faces of a cuboid specimen. It is seems reasonable to expect that the mechanical response of orthotropic materials in simple tension should be consistent with

1. the response of the composite in simple tension in the plane of the fibres is stiffer than the out-of-plane;

2. the composite should contract in the plane perpendicular to the direction of the applied force.

Although the first of these seems intuitively appealling, there is scant experimental evidence to support it, especially for soft tissue. What little evidence there is comes from the ultrasonic measurement of the stiffness matrices of orthotropic, angle-ply composites. The data of Hosten (1992) for an orthonormal PEEK-carbon fibre composite can be used to infer an in-plane Young's modulus of 66.7 GPa and a Young's modulus out of the plane of the fibres of 11.6 GPa. Kelly *et al.* (2005) carried out ultrasonic measurements on a series of composite laminates of glass fibres in a polypropylene matrix for a range of angle ply laminates, with laminate angles of ±0, 10, 20, 30 and 40°. For the ±20° laminate, for example, the Young's moduli in the plane of the fibres can be calculated to be 11.0 GPa and 31.3 GPa, while the out-of-plane Young's modulus is 10.4 GPa. In support of the second axiom, there have been no reports in the literature of arterial specimens expanding in directions orthogonal to the applied force in simple tension (so-called auxetic behaviour), particularly the large auxetic effects predicted here.

Even though the assumption that orthotropic materials depend only on the reduced I_1, I_4, I_6 basis of invariants significantly reduces the complexity of the constitutive law, it seems that a general analysis of their behaviour even for simple tension is not possible. This is true even for strain energies that are *separable* functions of I_1, I_4, I_6, i.e.,

$$W = f(I_1) + g(I_4) + g(I_6), \tag{1.1}$$

the strain-energy functions of interest here. Insight into their generic response can therefore only be gleaned from consideration of specific examples of such materials, with common features of the response then considered indicative of the general response. The Standard Reinforced Model proposed by Goriely and Tabor (2013) for purposes such as these is considered, as are specific instances of the influential HGO model for the mechanical response for the carotid arteries of rabbits proposed by Holzapfel *et al.* (2000, 2004). There are two notable surprising qualitative features of the mechanical response in simple tension that are common to all the models considered here:

1. the out-of-plane response can be stiffer than the in-plane over a finite range of strain;

2. even when the in-plane response is much stiffer than the out-of-plane, as might be expected, it is accompanied by a severe contraction in-plane and an pronounced *expansion* in the out-of-plane direction.

Unfortunately there seems to be no simple remedy. One approach might be to adopt the idea that the fibres do not support compression and that their contribution to the overall mechanical response should be neglected when they are under compression (Holzapfel and Ogden, 2015). This might be especially appropriate when modelling simple tension in the out-of-plane direction. However, it is shown that the adoption of this tension-compression switch can have only a marginal effect on the qualitative features of the mechanical response for all three simple tension modes.

Another remedial approach considered here is that, since the reduced models involving only the I_1, I_4, I_6 invariants don't recover the linear theory for the infinitesimal strain regime, the first necessary step towards models capable of predicting intuitive response in simple tension is to generalise the models (1.1) as simply as possible so that they *are* compatible with the linear theory. Immediate practical difficulties present themselves. Since the linear theory is a six-constant theory (Spencer, 1984; Destrade *et al.*, 2002), six independent experiments would appear necessary to obtain reliable models, the three simple tension experiments considered here being obvious candidates. Such a comprehensive suite of testing has not appeared in the literature, to the best of the authors' knowledge. Even with such an extensive database, the choosing of a strain energy that both fits the data and predicts realistic response in all aspects of these tests is a formidable, yet unavoidable, challenge. Another practical difficulty is that the generalisation proposed here assumes a dependence on the classical Rivlin invariants in a natural way. However, it is shown here that the material constants of the new model cannot always be easily interpreted in terms of material constants measured independently via experiments.

This suggests that an alternative formulation of the theory of orthotropic materials in terms of physically based invariants could be useful. For example, a set of invariants that

has an immediate physical interpretation for orthotropic materials has been proposed by Shariff (2011), with the material constants easily determined using triaxial tests. Due to space constraints here, formulations of the theory using physically based invariants will be considered elsewhere.

2   Preliminaries

The preliminaries are standard and those given by Horgan and Murphy (2016) are given for completeness. Let $\boldsymbol{F}, \boldsymbol{C} = \boldsymbol{F}^T \boldsymbol{F}, \boldsymbol{B} = \boldsymbol{F} \boldsymbol{F}^T$ denote the deformation gradient, right and left Cauchy-Green strain tensors respectively. Incompressible materials for which $\det \boldsymbol{F} = 1$ are of interest here. The general stress-strain law for incompressible, hyperelastic materials with a strain-energy function per unit undeformed volume W has the form

$$\boldsymbol{\sigma} = -p\boldsymbol{I} + 2\boldsymbol{F}\frac{\partial W}{\partial \boldsymbol{C}}\boldsymbol{F}^T, \qquad (2.1)$$

where p is an arbitrary scalar field and $\boldsymbol{\sigma}$ is the Cauchy stress. Spencer (1984) has proposed that the strain-energy function for a nonlinearly hyperelastic material with two preferred directions $\boldsymbol{M}, \boldsymbol{M}'$ in the undeformed configuration is an arbitrary function of $(\boldsymbol{M}.\boldsymbol{M}')^2$ and

$$I_1 = tr(\boldsymbol{C}), \quad I_2 = \frac{1}{2}\left[I_1^2 - tr\left(\boldsymbol{C}^2\right)\right], \quad I_4 = \boldsymbol{M}.\boldsymbol{C}\boldsymbol{M}, \quad I_5 = \boldsymbol{M}.\boldsymbol{C}^2\boldsymbol{M},$$
$$I_6 = \boldsymbol{M}'.\boldsymbol{C}\boldsymbol{M}', \quad I_7 = \boldsymbol{M}'.\boldsymbol{C}^2\boldsymbol{M}', \quad I_8 = \boldsymbol{M}.\boldsymbol{M}'\ \boldsymbol{M}.\boldsymbol{C}\boldsymbol{M}'. \qquad (2.2)$$

Since $\boldsymbol{M}.\boldsymbol{M}'$ is constant, many authors use the alternative invariant $\boldsymbol{M}.\boldsymbol{C}\boldsymbol{M}'$ instead of I_8 as used here. However, since it seems sensible to emphasise that the invariants are invariant under a change of sign in the preferred directions, I_8 as defined above is preferred here. When $\boldsymbol{M}.\boldsymbol{M}' = 0$, that is for initially orthogonal preferred directions, then $I_8 \equiv 0$ and there is therefore no constitutive dependence on this invariant. Although doubt has been cast on the completeness of this basis of invariants by Shariff and Bustamante (2015), who have concluded that only five of these invariants are independent, the classical formulation of the theory of orthotropic materials is considered here.

Noting that

$$\frac{\partial I_1}{\partial \boldsymbol{C}} = \boldsymbol{I}, \quad \frac{\partial I_2}{\partial \boldsymbol{C}} = I_1\boldsymbol{I} - \boldsymbol{C}, \quad \frac{\partial I_4}{\partial \boldsymbol{C}} = \boldsymbol{M} \otimes \boldsymbol{M}, \quad \frac{\partial I_5}{\partial \boldsymbol{C}} = \boldsymbol{M} \otimes \boldsymbol{C}\boldsymbol{M} + \boldsymbol{C}\boldsymbol{M} \otimes \boldsymbol{M},$$
$$\frac{\partial I_6}{\partial \boldsymbol{C}} = \boldsymbol{M}' \otimes \boldsymbol{M}', \quad \frac{\partial I_7}{\partial \boldsymbol{C}} = \boldsymbol{M}' \otimes \boldsymbol{C}\boldsymbol{M}' + \boldsymbol{C}\boldsymbol{M}' \otimes \boldsymbol{M}',$$
$$\frac{\partial I_8}{\partial \boldsymbol{C}} = \frac{1}{2}\boldsymbol{M}.\boldsymbol{M}'\left(\boldsymbol{M} \otimes \boldsymbol{M}' + \boldsymbol{M}' \otimes \boldsymbol{M}\right), \qquad (2.3)$$

the constitutive law for an incompressible, nonlinearly hyperelastic material with two preferred directions is therefore given by

$$\boldsymbol{\sigma} = -p\boldsymbol{I} + 2W_1\boldsymbol{B} + 2W_2\left(I_1\boldsymbol{B} - \boldsymbol{B}^2\right) + 2W_4\left(\boldsymbol{F}\boldsymbol{M} \otimes \boldsymbol{F}\boldsymbol{M}\right) +$$
$$2W_5\left(\boldsymbol{F}\boldsymbol{M} \otimes \boldsymbol{B}\boldsymbol{F}\boldsymbol{M} + \boldsymbol{B}\boldsymbol{F}\boldsymbol{M} \otimes \boldsymbol{F}\boldsymbol{M}\right) + 2W_6\left(\boldsymbol{F}\boldsymbol{M}' \otimes \boldsymbol{F}\boldsymbol{M}'\right) +$$
$$2W_7\left(\boldsymbol{F}\boldsymbol{M}' \otimes \boldsymbol{B}\boldsymbol{F}\boldsymbol{M}' + \boldsymbol{B}\boldsymbol{F}\boldsymbol{M}' \otimes \boldsymbol{F}\boldsymbol{M}'\right) + \boldsymbol{M}.\boldsymbol{M}'W_8\left(\boldsymbol{F}\boldsymbol{M} \otimes \boldsymbol{F}\boldsymbol{M}' + \boldsymbol{F}\boldsymbol{M}' \otimes \boldsymbol{F}\boldsymbol{M}\right),$$
$$(2.4)$$

where subscripts attached to W denote partial differentiation with respect to the appropriate invariant. It will be required that the strain energy and the stress vanish in the undeformed configuration. Consequently the following conditions will be assumed to hold:

$$W^0 = 0, \quad 2W_1^0 + 4W_2^0 = p^0, \quad W_4^0 + 2W_5^0 = 0, \quad W_6^0 + 2W_7^0 = 0, \quad W_8^0 = 0, \quad (2.5)$$

where the 0 superscript denotes evaluation in the undeformed configuration for which $I_1 = I_2 = 3$, $I_4 = I_5 = I_6 = I_7 = 1$, $I_8 = (\boldsymbol{M}.\boldsymbol{M'})^2$.

3 Simple tension tests

An important material characterisation test is simple tension of cuboid specimens, in which forces are only applied normal to two parallel faces of the specimens. It is assumed that two families of mechanically equivalent, initially straight fibres are embedded in an incompressible, nonlinearly elastic matrix. Choosing the origin of a Cartesian coordinate system to be the centre of the cuboid specimen, let the fibres have the following directions $\boldsymbol{M}$, $\boldsymbol{M'}$ in the reference configuration:

$$\boldsymbol{M} = C\boldsymbol{e}_x + S\boldsymbol{e}_y, \quad \boldsymbol{M'} = -C\boldsymbol{e}_x + S\boldsymbol{e}_y, \quad C \equiv \cos\Theta, \ S \equiv \sin\Theta,$$

with $\boldsymbol{e}_z$ normal to the plane of the fibres. Choose the x-axis as the bisector of the smaller of the angles between the two fibres, as illustrated in Figure 1. Then $\Theta \in \left(0, \frac{\pi}{4}\right]$. The two limiting cases of $\Theta = 0$ and $\Theta = \pi/4$ correspond to the cases of transverse isotropy and orthonormality respectively. This arrangement of the fibres and their assumed mechanical equivalence means that no shearing stresses are generated in the simple tension test considered here.

Let λ_x, λ_y, λ_z, with $\lambda_x\lambda_y\lambda_z = 1$ to ensure incompressibility, denote the principal stretches for simple tension. The invariants (2.2) with the arrangement of fibres as illustrated in Figure 1 have the form

$$I_1 = \lambda_x^2 + \lambda_y^2 + \lambda_z^2, \quad I_2 = \lambda_x^2\lambda_y^2 + \lambda_y^2\lambda_z^2 + \lambda_x^2\lambda_z^2, \quad I_4 = I_6 = \lambda_x^2 C^2 + \lambda_y^2 S^2,$$
$$I_5 = I_7 = \lambda_x^4 C^2 + \lambda_y^4 S^2, \quad I_8 = (C^2 - S^2)(\lambda_x^2 C^2 - \lambda_y^2 S^2). \quad (3.1)$$

The corresponding normal Cartesian components of the constitutive law (2.4) are therefore given by

$$\sigma_{xx} = -p + 2W_1\lambda_x^2 + 2W_2\lambda_x^2\left(\lambda_y^2 + \lambda_z^2\right) + 2(W_4 + W_6)\lambda_x^2 C^2 + 4(W_5 + W_7)\lambda_x^4 C^2$$
$$+ 2(C^2 - S^2)W_8\lambda_x^2 C^2,$$
$$\sigma_{yy} = -p + 2W_1\lambda_y^2 + 2W_2\lambda_y^2\left(\lambda_x^2 + \lambda_z^2\right) + 2(W_4 + W_6)\lambda_y^2 S^2 + 4(W_5 + W_7)\lambda_y^4 S^2$$
$$+ 2(S^2 - C^2)W_8\lambda_y^2 S^2,$$
$$\sigma_{zz} = -p + 2W_1\lambda_z^2 + 2W_2\lambda_z^2\left(\lambda_x^2 + \lambda_y^2\right). \quad (3.2)$$

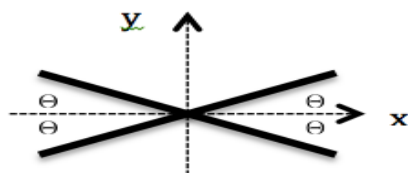Simple tension in each of the principal directions is now considered in turn.

Figure 1: The fibre arrangement.

3.1 Simple tension in the x-direction

For this test, $\sigma_{yy} = \sigma_{zz} = 0$ and (3.2) therefore yields

$$\sigma_{xx} = 2W_1\left(\lambda_x^2 - \lambda_z^2\right) + 2W_2\frac{1}{\lambda_x^2\lambda_z^2}\left(\lambda_x^2 - \lambda_z^2\right) + 2(W_4 + W_6)\lambda_x^2 C^2 + 4(W_5 + W_7)\lambda_x^4 C^2$$
$$+ 2(C^2 - S^2)W_8\lambda_x^2 C^2,$$
$$0 = W_1\lambda_x^2\lambda_z^2\left(1 - \lambda_x^2\lambda_z^4\right) + W_2\lambda_x^4\lambda_z^2\left(1 - \lambda_x^2\lambda_z^4\right) + (W_4 + W_6)\lambda_x^2\lambda_z^2 S^2 + 2(W_5 + W_7)S^2$$
$$+ (S^2 - C^2)W_8\lambda_x^2\lambda_z^2 S^2, \quad (3.3)$$

noting that $\lambda_y = \frac{1}{\lambda_x\lambda_z}$. The second of these therefore can be used to determine λ_z in terms of λ_x and the first to determine σ_{xx} as a function of λ_x.

3.2 Simple tension in the y-direction

Setting $\sigma_{xx} = \sigma_{zz} = 0$ in (3.2) yields

$$\sigma_{yy} = 2W_1\left(\lambda_y^2 - \lambda_z^2\right) + 2W_2\lambda_x^2\left(\lambda_y^2 - \lambda_z^2\right) + 2(W_4 + W_6)\lambda_y^2 S^2 + 4(W_5 + W_7)\lambda_y^4 S^2$$
$$+ 2(S^2 - C^2)W_8\lambda_y^2 S^2,$$
$$0 = W_1\lambda_y^2\lambda_z^2\left(1 - \lambda_y^2\lambda_z^4\right) + W_2\lambda_y^4\lambda_z^2\left(1 - \lambda_y^2\lambda_z^4\right) + (W_4 + W_6)\lambda_y^2\lambda_z^2 C^2 + 2(W_5 + W_7)C^2$$
$$+ (C^2 - S^2)W_8\lambda_y^2\lambda_z^2 C^2. \quad (3.4)$$

The second of these therefore can be used to determine λ_z in terms of λ_y and the first to determine σ_{yy} as a function of λ_y.

3.3 Simple tension in the z-direction

Setting $\sigma_{xx} = \sigma_{yy} = 0$ in (3.2) yields

$$\sigma_{zz} = 2W_1\left(\lambda_z^2 - \lambda_x^2\right) + 2W_2\lambda_y^2\left(\lambda_z^2 - \lambda_x^2\right) - 2(W_4 + W_6)\lambda_x^2 C^2 - 4(W_5 + W_7)\lambda_x^4 C^2$$
$$+ 2(S^2 - C^2)W_8\lambda_x^2 C^2,$$
$$0 = (W_1 + \lambda_z^2 W_2)(\lambda_y^2 - \lambda_x^2) + (W_4 + W_6)(\lambda_y^2 S^2 - \lambda_x^2 C^2) + 2(W_5 + W_7)(\lambda_y^4 S^2 - \lambda_x^4 C^2) +$$
$$(S^2 - C^2)W_8(\lambda_y^2 S^2 + \lambda_x^2 C^2). \quad (3.5)$$

The second of these and the incompressibility condition $\lambda_x\lambda_y\lambda_z = 1$ determine λ_x, λ_y in terms of the out-of-plane principal stretch λ_z and hence σ_{zz} can be considered a function only of λ_z.

The analysis of even simple tension experiments is self-evidently formidable for orthotropic materials and it doesn't seem that much progress can be made in general. To simplify the analysis, while at the same time hoping to capture the significant effects of anisotropy on the mechanical response, assumptions are typically made on the form of the strain-energy function. A popular reduced model for modelling soft tissue has the form

$$W = f(I_1) + g(I_4) + g(I_6), \quad (3.6)$$

where, to satisfy the initial conditions (2.5),

$$f(3) + 2g(1) = 0, \quad 2f'(3) = p^0, \quad g'(1) = 0. \quad (3.7)$$

Although, as observed by Murphy (2014), the corresponding linear model is not fully recovered on restriction to infinitesimal deformations, these reduced models simplify the complexity of the stress-strain relation significantly with simple tension in the x-, y- and z-directions now described respectively by

$$\sigma_{xx} = 2f'(I_1)\left(\lambda_x^2 - \lambda_z^2\right) + 4g'(I_4)\lambda_x^2 C^2, \quad 0 = f'(I_1)\left(1 - \lambda_x^2\lambda_z^4\right) + 2g'(I_4)S^2,$$

$$\sigma_{yy} = 2f'(I_1)\left(\lambda_y^2 - \lambda_z^2\right) + 4g'(I_4)\lambda_y^2 S^2, \quad 0 = f'(I_1)\left(1 - \lambda_y^2\lambda_z^4\right) + 2g'(I_4)C^2,$$

$$\sigma_{zz} = 2f'(I_1)\left(\lambda_z^2 - \lambda_x^2\right) - 4g'(I_4)\lambda_x^2 C^2,$$
$$0 = f'(I_1)(1 - \lambda_x^4\lambda_z^2) + 2g'(I_4)(S^2 - \lambda_x^4\lambda_z^2 C^2), \tag{3.8}$$

noting that $g'(I_4) = g'(I_6)$ for simple tension. However, even with this simplification, little progress can be made analytically to explore the relationship between the stress and the corresponding principal stretches.

4 A simple model

It seems that the form of the strain energy must be specified before further progress can be made. It makes sense initially to consider a prototype strain-energy function that balances simplicity of form with an acceptable variety of mechanical response. The Standard Material for orthotropic materials has the form

$$W = \gamma_1\left(I_1 - 3\right) + \gamma_2\left(I_4 - 1\right)^2 + \gamma_2\left(I_6 - 1\right)^2, \quad \gamma_1, \gamma_2 > 0. \tag{4.1}$$

Some interesting features of the mechanical response of this material are discussed in Goriely and Tabor (2013). The Standard Material is the simplest polynomial form of the reduced strain energy (3.6) that is consistent with the initial conditions (3.7) and is a simple generalisation of the neo-Hookean isotropic strain energy for orthotropic materials. Substitution into (3.8) yields, for simple tension in the x-, y- and z-directions respectively,

$$\hat{\sigma}_{xx} = \lambda_x^2 - \lambda_z^2 + \lambda_x^2\cot^2\Theta\left(\lambda_x^2\lambda_z^4 - 1\right),$$
$$0 = \frac{1}{\lambda_x^2\lambda_z^2} - \lambda_z^2 + \gamma\left(\lambda_x^2 C^2 + \frac{S^2}{\lambda_x^2\lambda_z^2} - 1\right)\frac{S^2}{\lambda_x^2\lambda_z^2},$$

$$\hat{\sigma}_{yy} = \lambda_y^2 - \lambda_z^2 + \lambda_y^2\tan^2\Theta\left(\lambda_y^2\lambda_z^4 - 1\right),$$
$$0 = \frac{1}{\lambda_y^2\lambda_z^2} - \lambda_z^2 + \gamma\left(\frac{C^2}{\lambda_y^2\lambda_z^2} + \lambda_y^2 S^2 - 1\right)\frac{C^2}{\lambda_y^2\lambda_z^2},$$

$$\hat{\sigma}_{zz} = \lambda_z^2 - \lambda_x^2 + \frac{\lambda_x^2\left(1 - \lambda_x^4\lambda_z^2\right)}{\tan^2\Theta - \lambda_x^4\lambda_z^2},$$
$$0 = \frac{1}{\lambda_x^2\lambda_z^2} - \lambda_x^2 + \gamma\left(\lambda_x^2 C^2 + \frac{S^2}{\lambda_x^2\lambda_z^2} - 1\right)\left(\frac{S^2}{\lambda_x^2\lambda_z^2} - \lambda_x^2 C^2\right), \tag{4.2}$$

assuming that $\tan\Theta \neq \lambda_x^2\lambda_z$. Here $\hat{\sigma} \equiv \frac{\sigma}{2\gamma_1}$ and $\gamma \equiv \frac{4\gamma_2}{\gamma_1}$ is a measure of the anisotropy of the material, with increasing values of γ corresponding to a stiffening of the fibres, for example.

Two specific forms for the Standard Reinforcing model will be used for illustrative purposes: a moderately anisotropic model with $\gamma = 1$ and a stiffer version with $\gamma = 10$. In both cases $\Theta = 40°$. For each of $(4.2)_2$, $(4.2)_4$ and $(4.2)_6$, the non-axial strain was determined from specified values of the axial strain (see the Appendix for details). The stress-stretch plots for simple tension in each of the orthogonal principal directions are given in Figure 2.
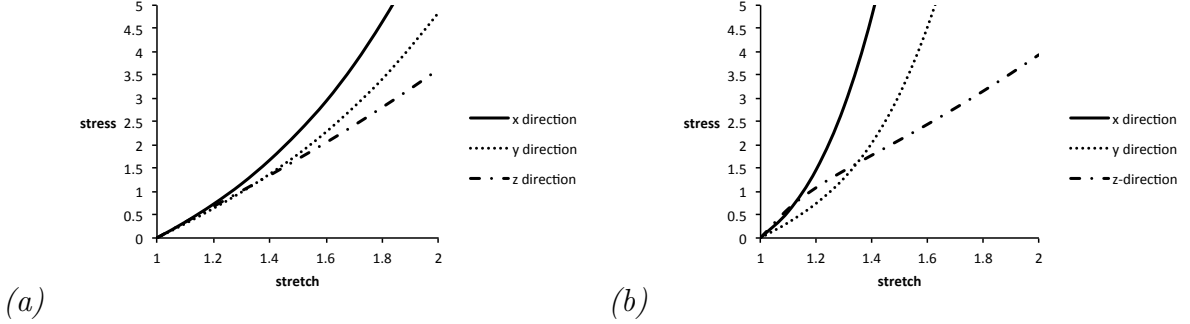

(a)   (b)

Figure 2: Simple tension plots for the Standard Model (4.1) in the three orthogonal principal directions for $\Theta = 40°$. In (a) $\gamma = 1$, with $\gamma = 10$ in (b). Although in both cases the infinitesimal Young's modulus is greater in the z-direction, the in-plane modes eventually become stiffer than the out-of-plane. The out-of-plane mode can be stiffer, however, than the y mode for a moderate range of strain for stiff fibres.

Although it can be shown that the infinitesimal Young's modulus in the z-direction is greater than those in the in-plane principal directions, the plots show that the planar response eventually becomes stiffer, as might be intuitively expected. There are still some noteworthy unexpected qualitative features, however. The first is that for moderately anisotropic materials, with $\gamma = 1$, the stress in each of the principal directions is of the same order of magnitude for strains of 100%. For strongly anisotropic materials, here represented by choosing $\gamma = 10$, the weaker of the two in-plane responses is still weaker than the out-of-plane response in the z-direction for strains up to 30% and the response in the both the x- and z-directions are virtually identical for strains up to 15%. In all the simulations reported here, and in what follows, strain controlled experiments are envisaged, with 2 being the maximum axial stretch allowed. It is expected that such a strain regime should include the strain experienced by soft tissue in physiological conditions, even if one were to include residual strains. It is worth noting that strain-energy functions are sometimes proposed for the mechanical response of arteries without any explicit indication as to the range of stress or strain for which they are considered apt.

Even when the stress-stretch response seems consistent with our expectations of how a fibre-reinforced composite should behave, such as strains above 70% for strongly anisotropic materials in Figure 2(b), other problems with the constitutive model for simple tension in the x-direction are evident in Figure 3.
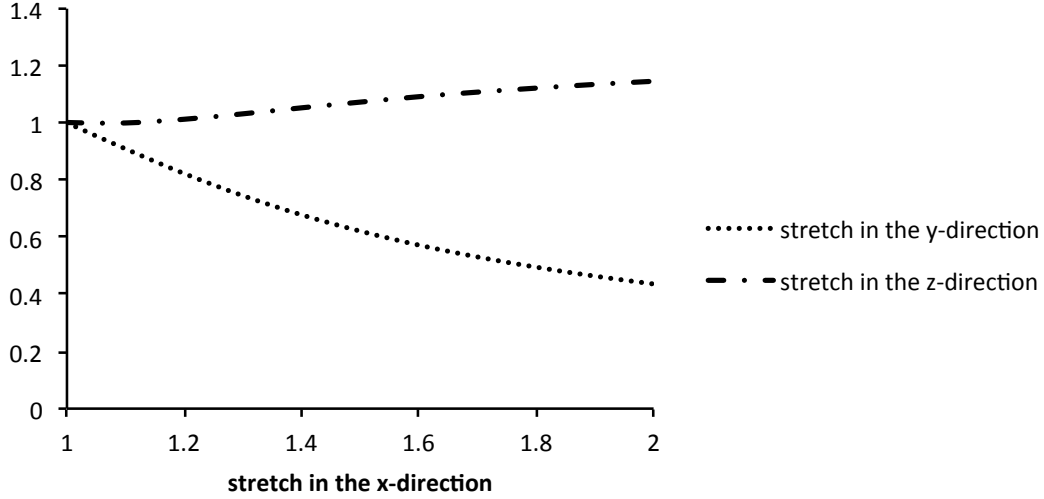
Figure 3: Plots of the principal stretches as a function of the stretch in the x-direction for simple tension in the x-direction for the Standard Model (4.1) with $\gamma = 10$ and $\Theta = 40°$. Note the *positive* Poisson effect in the z-direction, i.e, the specimen is expected to expand in the out-of-plane direction.

Instead of a contraction in each of the two directions orthogonal to the x-direction, as might be expected, there is a pronounced *expansion* in the out-of-plane direction for precisely those stretches for which the stress-stretch responses seem acceptable, accompanied by an extreme contraction in the y-direction. Thus at large axial stretches, thin plates in the x-y plane are predicted to warp to form thin plates in the x-z plane. This seems unphysical, with no reports of such behaviour in the literature, as far as the authors are aware.

5   Models of arterial response

It was shown in the last section that the mechanical response in simple tension of the Standard Model seems counterintuitive, with essentially two mutually exclusive qualitative modes of response:

1. the in-plane mode of simple tension is stiffer than the out-of-plane but at the expense of a significant negative Poisson's effect;

2. the material contracts in directions orthogonal to the direction of the applied force but now the out-of-plane direction is stiffer than the the in-plane response.

It will be shown that these modes also seem characteristic of the separable models (3.6) that are often used to model the mechanical response of large, elastic arteries.

  An influential separable model of the mechanical response of arteries was proposed

10

by Holzapfel *et al.* (2000) and has the form

$$W = \frac{c}{2}\left(I_1 - 3\right) + \frac{k_1}{2k_2} \sum_{i=4,6} \{\exp\left[k_2\left(I_i - 1\right)^2\right] - 1\}. \tag{5.1}$$

where $c, k_1 > 0$ are stress-like material parameters and $k_2 > 0$ is a dimensionless parameter. The Standard Model (4.1) considered previously is a special case, obtained by letting $k_2 \to 0$. It follows therefore that for this material

$$W_1 = c/2, \quad W_4 + W_6 = 2k_1\left(I_4 - 1\right)\exp k_2\left(I_4 - 1\right)^2, \tag{5.2}$$

with I_4 given in (3.1). Substituting these terms into (3.8) yields the following determining equations for simple tension in the x-, y- and z-direction respectively:

$$\bar{\sigma}_{xx} = \lambda_x^2 - \lambda_z^2 + \lambda_x^2 \cot^2\Theta\left(\lambda_x^2\lambda_z^4 - 1\right),$$
$$0 = c\left(1 - \lambda_x^2\lambda_z^4\right) + 4k_1 S^2\left(\lambda_x^2 C^2 + \lambda_y^2 S^2 - 1\right)\exp k_2\left(\lambda_x^2 C^2 + \lambda_y^2 S^2 - 1\right)^2,$$

$$\bar{\sigma}_{yy} = \lambda_y^2 - \lambda_z^2 + \lambda_y^2 \tan^2\Theta\left(\lambda_y^2\lambda_z^4 - 1\right),$$
$$0 = c\left(1 - \lambda_y^2\lambda_z^4\right) + 4k_1 C^2\left(\lambda_x^2 C^2 + \lambda_y^2 S^2 - 1\right)\exp k_2\left(\lambda_x^2 C^2 + \lambda_y^2 S^2 - 1\right)^2,$$

$$\bar{\sigma}_{zz} = c\left(\lambda_z^2 - \lambda_x^2\right) - 4k_1\lambda_x^2 C^2\left(\lambda_x^2 C^2 + \lambda_y^2 S^2 - 1\right)\exp k_2\left(\lambda_x^2 C^2 + \lambda_y^2 S^2 - 1\right)^2,$$
$$0 = c(1 - \lambda_x^4\lambda_y^2) + 4k_1(S^2 - \lambda_x^4\lambda_z^2 C^2)\left(\lambda_x^2 C^2 + \lambda_y^2 S^2 - 1\right)\exp k_2\left(\lambda_x^2 C^2 + \lambda_y^2 S^2 - 1\right)^2, \tag{5.3}$$

where $\bar{\sigma} \equiv \sigma/c$. Three random, specific instances of this model are now considered.

5.1 The HGO model

Holzapfel *et al.* (2000) fitted the HGO model (5.1) to experimental data of Fung *et al.* (1979) for extension and internal inflation of tubular arterial segments on carotid arteries of rabbits using the Levenberg-Marquardt algorithm to obtain the following parameters for the media:

$$c = 3\,\text{kPa}, \quad k_1 = 2.3632\,\text{kPa}, \quad k_2 = 0.8393, \quad \Theta = 29°. \tag{5.4}$$

Solving each of the sub-systems of equations (5.3) for these parameter values yields the simple tension-axial stretch relation in the appropriate direction. The results are summarised in the plots of Figure 4, where the stress in each case has been non-dimensionalised with respect to c.
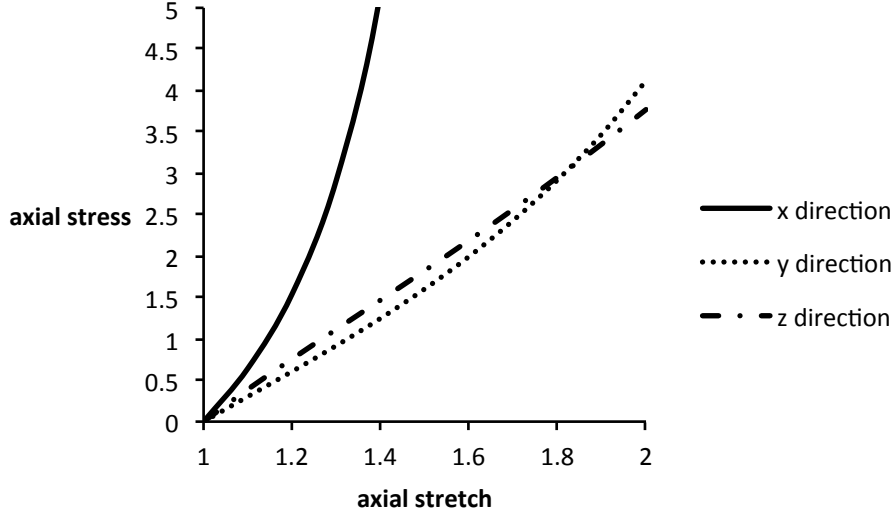
Figure 4: Plots of non-dimensional stress against axial stretch for each of the three principal directions for the HGO model (5.1), (5.4). Although the differences between the in-plane x-direction and the out-of-plane responses seem intuitively reasonable, the in-plane y response is virtually identical to the out-of-plane. Thus the material behaves as if it were *transversely isotropic* and not orthotropic as per design.

Based on the evidence from simple tension experiments alone, it would seem that the material (5.1), (5.4) is essentially *transversely isotropic* in the x-direction, despite the fact that the material was assumed orthotropic. Even if orthotropy were still claimed for this model, it is seems unlikely that the out-of-plane response is stiffer than one of the in-plane modes for much of the reported range of axial stretch. Figure 4 therefore displays the same unexpected features of the stress-stretch plots encountered earlier. Although the stress-stretch plot for the x-direction is much stiffer than those predicted for the other two, as might be expected, this behaviour is accompanied by unexpected stretches in the directions orthogonal to the direction of the applied force. These stretches are plotted in Figure 5 as a function of the axial stretch for simple tension in the x-direction. The most arresting feature of these plots is the changing nature of the out-of-plane stretch. Following an expected contraction, the material *expands* in the out-of-plane direction after an axial stretch of approximately 1.6. This is the stretch range for which the the material is finally an order of magnitude stiffer in the x-direction than in the out-of-plane direction. Thus, as for the Standard Material, it seems that the material (5.1) can only achieve the necessary stiffness in the x-direction at the expense of auxetic out-of-plane stretches of the same order of magnitude as the axial stretch. Also note that the auxetic out-of-plane stretch, and the corresponding extreme contraction in the y-direction, are more pronounced at the upper range of axial stretch considered here than for the Standard Material. At large values of axial stretch for simple tension in the x-direction, therefore, the HGO model with parameters (5.4) predicts a warping of cuboid specimens, with of example, thin specimens in the x-y plane being transformed into thin sheets in the x-z plane.
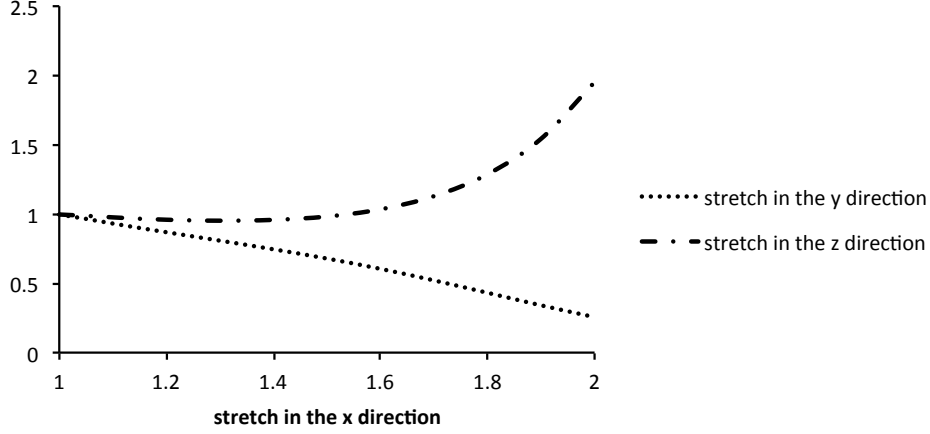
Figure 5: The stretches in the y- and z-directions as a function of axial stretch for simple tension in the x-direction. Note the dramatic increase in the auxetic effect in the out-of-plane direction and the severe contraction in the y-direction after initially behaving in a physically realistic manner.

5.2 An orthonormal example

The HGO model (5.1) was used by Holzapfel *et al.* (2004) to fit the subset of experimental data of Chuong and Fung (1983) labelled '81:2' on the adventitia of a carotid artery harvested from a rabbit. They obtained the following parameters:

$$c = 1.1068\,\text{kPa}, \quad k_1 = 5.3822\,\text{kPa}, \quad k_2 = 0.6020, \quad \Theta = 45°. \tag{5.5}$$

There is a good fit of the model to the data, the fibre angle is in the middle of the range of the angles obtained by Holzapfel *et al.* (2004) and the anisotropic parameter k_1 is much larger than the isotropic parameter c, in keeping with the intuitive expectation that the fibres are much stiffer than the matrix in which they are embedded.

For orthonormal materials such as this, where the two families of fibres are at right angles in the reference configuration, there is only one in-plane response in simple tension. The simple tension responses in-plane and out-of-plane can be obtained by substituting the parameter values (5.5) into (5.3) and are tabulated in the Appendix. A graphical summary of these responses is given in the Figure 6. The same constitutive quirks of the HGO model (5.1) noted for its previous implementation are evident here. This model of the carotid artery is stronger out of the plane of the fibres for strains up to 35%. The in-plane response isn't an order of magnitude bigger than the in-plane, as might be expected, until about 80% strain. However this order of magnitude difference in stiffness is accompanied by a large auxetic effect, as can be seen from the plot of λ_y, λ_z against the axial stretch for simple tension in the x-direction given in Figure 7.

13
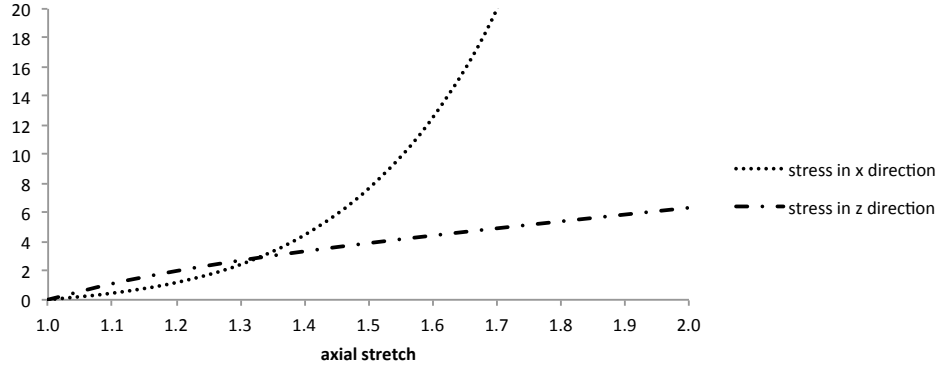
Figure 6: Although the in-plane response eventually becomes stiffer than the out-of-plane, it is seen that the composite is stiffer out of the plane for strains up to 30%.
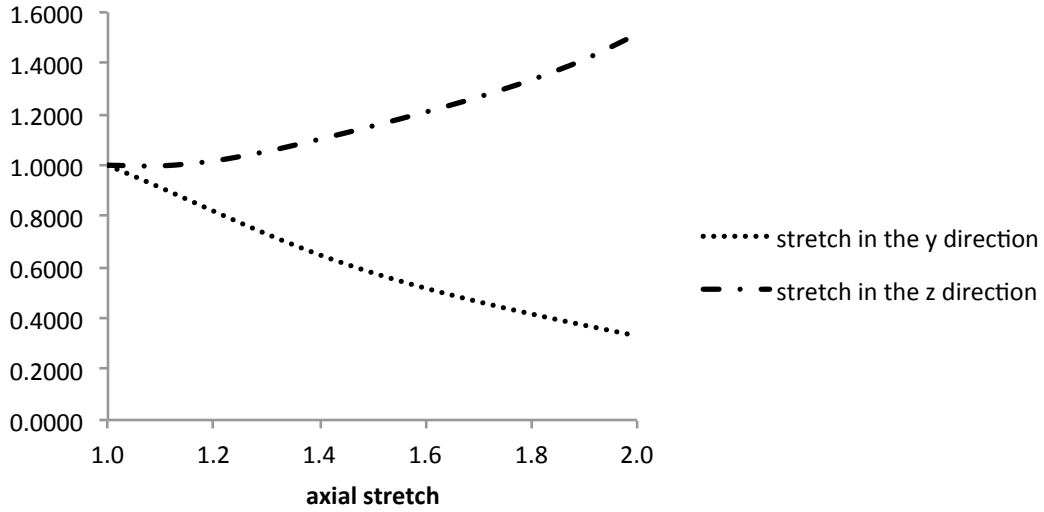
Figure 7: Plots of the non-axial principal stretches as a function of the stretch in the x-direction for simple tension in the x-direction. Note the *positive* Poisson effect in the z-direction, i..e, the specimen is expected to expand in the out-of-plane direction, and that this auxetic effect is significant with an expansion of approximately 50% for an axial strain of 100%.

14

5.3 A recent implementation

To characterise the local anisotropic mechanical response of intact aortic tissue, Gültekin *et al.* (2016) used the HGO model (5.1) with the following model parameters:

$$c = 16.95\text{kPa}, \quad k_1 = 243.57\text{kPa}, \quad k_2 = 2.57, \quad \Theta = 44.5°. \tag{5.6}$$

The predicted mechanical response in simple tension is given in tabular form in the Appendix and is summarised graphically here. The tension-axial stretch relations for the three directions are given in Figure 8. The same qualitative features identified previously for the other implementations of the HGO model (5.1) are present here with the out-of-plane stiffness larger than the in-plane for stretches up to approximately 30%, which could be physiologically relevant. When the in-plane stiffness is an order of magnitude larger than the out-of-plane, there is an auxetic out-of-plane stretch response as before, with the effect here especially pronounced as can be seen in Figure 9.

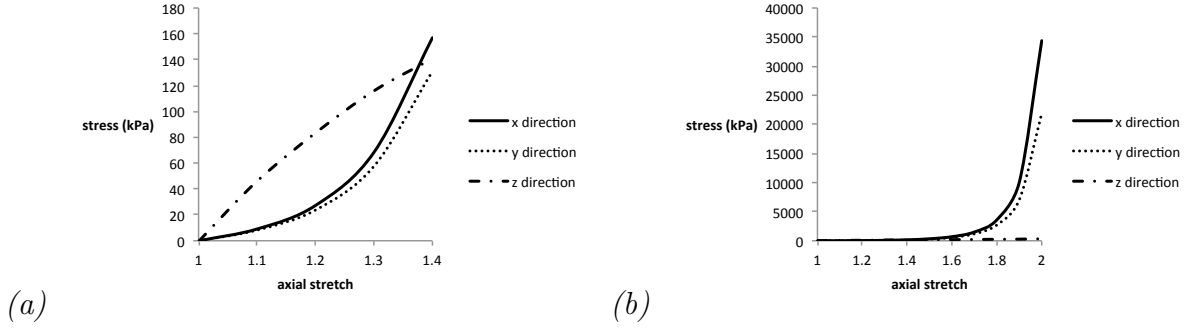(a)   (b)

Figure 8: Simple tension plots for the HGO model (5.1) for the parameters of Gültekin *et al.* (2016). Figure *(a)* details the mechanical response for small to moderate strains; in *(b)* the usual stretch range is plotted. The greater *out-of-plane* stiffness for stretches up to 35% is surprising.
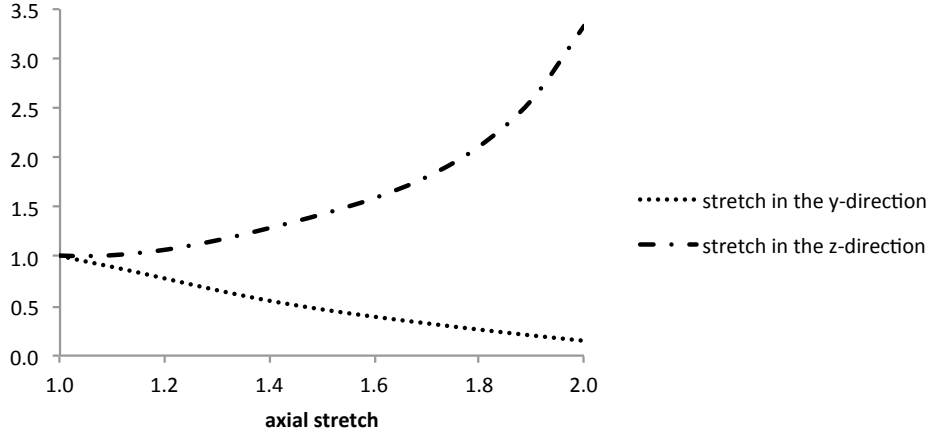
Figure 9: The stretches in the y- and z-directions as a function of axial stretch for simple tension in the x-direction. The auxetic effect in the out-of-plane direction is especially pronounced.

6 Fibre stretch

A possible remedy for the unexpected and unusual behaviour identified in the previous analysis while maintaining the I_1, I_4, I_6 form for the strain energy is to adopt the concept of a tension-compression switch, advocated by Holzapfel and Ogden (2015). The idea is that the fibres do not support compression and that their contribution to the overall mechanical response should be neglected when they are under compression. It might be anticipated that this could have a significant impact on the out-of-plane simple tension response, since an in-plane contraction of the matrix in response to the axial expansion should also contract the fibres. The approach adopted here to extract this isotropy from the underlying anisotropic assumption is to assume anisotropy *ab inito* and calculate I_4, the square of the fibre stretch, for the full range of the axial stretch used here. If $I_4 < 1$ at any axial stretch, then isotropy is assumed instead and the corresponding stress and remaining principal stretches are re-calculated. This procedure will now be implemented for the influential HGO model (5.1), (5.4).

For this model the in-plane fibres contract for simple tension in the out-of-plane direction and so, if the tension-compression switch were used, the out-of-plane mode of simple tension would be isotropic. However, as can be seen from Figure 10, there is very little difference between the two out-of-plane modes and the response in the y direction. It seems that describing the material as transversely isotropic over the range of axial strain employed would be a useful summary of the material response in simple tension, independent of whether or not the tension-compression switch is used as a constitutive assumption.

There is another constitutive oddity worth noting for the original HGO model (5.1), (5.4). The fibres *decrease* fractionally in length by about 1% when the material is stretched in the y-direction for axial stretches in the range $[1, 1.4]$. Beyond this range, the fibres lengthen in response to increased axial stretch. If the tension-compression switch were employed, there is only an infinitesimal change in the stress-stretch response in the y-direction and the anisotropic response given in Figure 10. The large auxetic effect noted
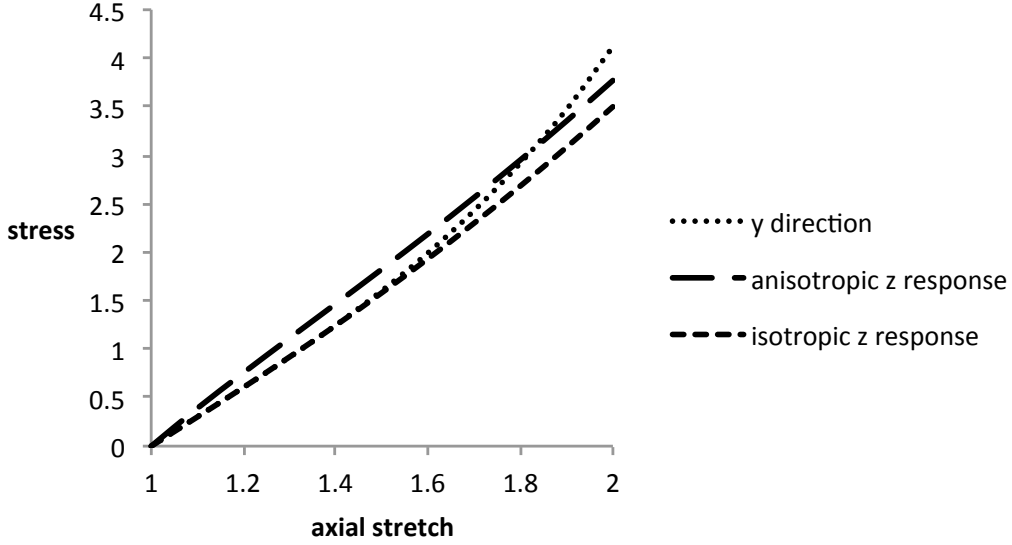
Figure 10: Out-of-plane simple tension when the material is assumed (1) anisotropic and (2) isotropic, with the tension-compression switch employed. The corresponding y mode is also shown for comparative purposes. The anisotropic out-of-plane response is slightly stiffer than the isotropic. Either is well-approximated by the in-plane y mode.

earlier that is seemingly characteristic of simple tension in the x-direction for separable materials of the form (3.6) will not be affected by the use of the tension-compression switch as simple tension in the x-direction is always accompanied by an increase in fibre length.

7 A compatible strain-energy function

It is hypothesised here that the undesirable behaviour illustrated in simple tension for models that depend only on separable functions of the I_1, I_4, I_6 invariants could be as a result of the non-recovery of the linear theory on restriction to infinitesimal deformations. For simple tension of orthotropic materials, there are nine obvious material constants that could be measured experimentally: the three Young's moduli and the six Poisson's ratios, two for each mode of simple tension. However, only three of these material constants are independent, as demonstrated in Horgan and Murphy (2016), for example. It is easy to show that the HGO model (5.1), and therefore its special case the Standard Model (4.1), is only a two constant model, on restriction to small strains. Thus these models cannot model the three modes of simple tension considered here, even for infinitesimal deformations.

One remedy that could be considered is to generalise the HGO model so that recovery of the full linear theory is possible for small strains. The linearised stress-strain relation

can be rewritten in the form

$$\boldsymbol{\sigma} = -p\boldsymbol{I} + m_1\boldsymbol{\epsilon} + (m_2\epsilon_M + m_3\epsilon_{M'} + 2m_4\boldsymbol{M}.\boldsymbol{M}'\epsilon_{MM'})\,\boldsymbol{M}\otimes\boldsymbol{M}$$
$$+ (m_3\epsilon_M + m_2\epsilon_{M'} + 2m_4\boldsymbol{M}.\boldsymbol{M}'\epsilon_{MM'})\,\boldsymbol{M}'\otimes\boldsymbol{M}' +$$
$$+ m_5\left(\boldsymbol{M}\otimes\boldsymbol{\epsilon M} + \boldsymbol{\epsilon M}\otimes\boldsymbol{M} + \boldsymbol{M}'\otimes\boldsymbol{\epsilon M}' + \boldsymbol{\epsilon M}'\otimes\boldsymbol{M}'\right),$$
$$+ \boldsymbol{M}.\boldsymbol{M}'(m_4\left(\epsilon_M + \epsilon_{M'}\right) + m_6\boldsymbol{M}.\boldsymbol{M}'\epsilon_{MM'})\left(\boldsymbol{M}\otimes\boldsymbol{M}' + \boldsymbol{M}'\otimes\boldsymbol{M}\right). \qquad (7.1)$$

where

$$m_1 \equiv 4(W_1^0 + W_2^0),$$
$$m_2 \equiv 4\left(W_{44}^0 + 4W_{45}^0 + 4W_{55}^0\right) = 4\left(W_{66}^0 + 4W_{67}^0 + 4W_{77}^0\right),$$
$$m_3 \equiv 4\left(W_{46}^0 + 2W_{47}^0 + 2W_{56}^0 + 4W_{57}^0\right),$$
$$m_4 \equiv 2\left(W_{48}^0 + 2W_{58}^0\right) = 2(W_{68}^0 + 2W_{78}^0),$$
$$m_5 \equiv 4W_5^0 = 4W_7^0,$$
$$m_6 \equiv 2W_{88}^0. \qquad (7.2)$$

The linearised theory is therefore a six constant theory (Spencer, 1984) and a comprehensive suite of experiments must be conducted to determine these material constants; the most efficient and practical method of determining these constants remains to be decided, especially for soft tissue. For the HGO model (5.1), it follows trivially that $m_3 = m_4 = m_5 = m_6 = 0$ and, wanting to generalise this model so that it is consistent with the linear theory while seeking as simple a form as possible, the following strain energy seems a natural choice:

$$W = c_1\left(I_1 - 3\right) + \frac{c_2}{2k_2}\{\exp\left[k_2\left(I_4 - 1\right)^2\right] + \exp\left[k_2\left(I_6 - 1\right)^2\right] - 2\}$$
$$+ c_3\left(I_4 I_6 - I_4 - I_6 + 1 - 2\right) + 2c_4\left(I_8 - I_8^0\right)\left(I_4 + I_6 - 2\right)$$
$$+ c_5\left(I_5 + I_7 - 2I_4 - 2I_6 + 2\right) + c_6\left(I_8 - I_8^0\right)^2. \qquad (7.3)$$

This form also ensures that the initial conditions (2.5) are identically satisfied. The material constants of the linearised theory are therefore

$$m_1 = 4c_1, \quad m_2 = 4c_2 \quad m_3 = 4c_3, \quad m_4 = 4c_4, \quad m_5 = 4c_5, \quad m_6 = 4c_6. \qquad (7.4)$$

It was shown in Horgan and Murphy (2016) that a strain-energy function is positive semi-definite for infinitesimal strains of an orthotropic, incompressible material if, and only if,

$$3m_1^2 + 8m_1 m_5 + 16C^2 S^2 m_5^2 + 8C^2 S^2 \hat{m} m_5 + 16(\boldsymbol{M}.\boldsymbol{M}')^2 C^4 S^4 \hat{m} m_6 +$$
$$2(\boldsymbol{M}.\boldsymbol{M}')^2(1 + C^4 + S^4)m_1 m_6 + 8C^2 S^2 (\boldsymbol{M}.\boldsymbol{M}')^2 m_5 m_6 + 4(C^4 + S^4 - C^2 S^2)m_1\hat{m} +$$
$$16(\boldsymbol{M}.\boldsymbol{M}')^2 m_1 m_4 + 32(\boldsymbol{M}.\boldsymbol{M}')^2 C^2 S^2 m_4 m_5 - 64(\boldsymbol{M}.\boldsymbol{M}')^2 C^4 S^4 m_4^2 > 0, \qquad (7.5)$$

where $\hat{m} \equiv m_2 + m_3$, and

$$2\mu_{xy} = \frac{\sigma_{xy}}{\epsilon_{xy}} = m_1 + 4(m_2 - m_3)C^2 S^2 + 2m_5 > 0,$$
$$2\mu_{xz} = \frac{\sigma_{xz}}{\epsilon_{xz}} = m_1 + 2m_5 C^2 > 0, \quad 2\mu_{yz} = \frac{\sigma_{yz}}{\epsilon_{yz}} = m_1 + 2m_5 S^2 > 0, \qquad (7.6)$$

18

using an obvious notation for the infinitesimal shear moduli. In view of (7.4), a straightforward replacement of the m_i constants by the c_i constants gives the corresponding necessary positive semi-definite restrictions on the constants for the new proposed model. It is anticipated that the determination of these constants from a full range of material characterisation tests will result in values for the material constants that automatically satisfy these restrictions.

It follows immediately from (7.4) and (7.6) that the material constants $c_1, c_2 - c_3, c_5$ have an immediate interpretation in terms of the infinitesimal shear moduli, i.e.,

$$2c_1 = \frac{\mu_{xz}S^2 - \mu_{yz}C^2}{S^2 - C^2}, \quad 8(c_2 - c_3) = \frac{\mu_{xy}\left(S^2 - C^2\right) + \mu_{xz}C^2 - \mu_{yz}S^2}{C^2S^2\left(S^2 - C^2\right)}, \quad 4c_5 = \frac{\mu_{yz} - \mu_{xz}}{S^2 - C^2}.$$

(7.7)

Interpretation of the other material constants in terms of other physical constants is much more problematic. Simple tension experiments have been the focus here and therefore it is pertinent to relate the material constants of (7.3) to the physical constants typically measured in these experiments. One approach is to relate the remaining material constants to appropriately defined Poisson's ratios and this have proved simpler than using the corresponding Young's moduli. For simple tension in the x-direction, for example, define the Young's modulus in the x-direction to be $E_x \equiv \frac{\sigma_{xx}}{\epsilon_{xx}}$ and the corresponding Poisson's ratios in the y- and z-directions to be $\nu_{xy} \equiv -\frac{\epsilon_{yy}}{\epsilon_{xx}}, \nu_{xz} \equiv -\frac{\epsilon_{zz}}{\epsilon_{xx}}$. The quantities E_y, E_z, ν_{yx}, ν_{yz}, ν_{zx}, ν_{zy} are defined similarly. Using the linear stress-strain relation (7.1), Horgan and Murphy (2016) obtained the following relations between the constants of the linear theory m_i and the appropriate Poisson's ratios:

$$\nu_{xy} = \frac{m_1 + 2(\hat{m} - m_6(\boldsymbol{M}.\boldsymbol{M}')^2)C^2S^2}{2(m_1 + 2m_5S^2 + (\hat{m} + 4m_4\boldsymbol{M}.\boldsymbol{M}' + m_6(\boldsymbol{M}.\boldsymbol{M}')^2)S^4)},$$

$$\nu_{yx} = \frac{m_1 + 2(\hat{m} - m_6(\boldsymbol{M}.\boldsymbol{M}')^2)C^2S^2}{2(m_1 + 2m_5C^2 + (\hat{m} - 4m_4\boldsymbol{M}.\boldsymbol{M}' + m_6(\boldsymbol{M}.\boldsymbol{M}')^2)C^4)},$$

$$\nu_{zx} = \frac{m_1 + 4m_5S^2 + 2(\hat{m} + 4m_4\boldsymbol{M}.\boldsymbol{M}' + m_6(\boldsymbol{M}.\boldsymbol{M}')^2)S^4 - 2(\hat{m} - m_6(\boldsymbol{M}.\boldsymbol{M}')^2)C^2S^2}{2\left(m_1 + 2m_5 + 4m_4\boldsymbol{M}.\boldsymbol{M}'(S^4 - C^4) + m_6(\boldsymbol{M}.\boldsymbol{M}')^2 + \hat{m}(S^2 - C^2)^2\right)},$$

(7.8)

with the corresponding relations for the material constants c_i obtained by again replacing m_i by c_i. Although these relations can be inverted to obtain the material constants $c_2 + c_3, c_4, c_6$ in terms of the Poisson's ratios and shear moduli, the analysis is tedious and not instructive. Indeed the relative difficulty in deriving correspondences between the material constants of (7.3) and the physical constants associated with simple tension suggests that the classical invariants (2.2) might not be the most convenient in modelling these tests. A more radical approach would be to use physically-based invariants to circumvent this problem. Proposals for such an approach have been been advocated by Shariff (2011) and Shariff (2016), for example; however, this alternative approach is not considered here.

Acknowledgements

This version of the paper incorporates many of the suggestions and ideas of the two anonymous reviewers and editor. We are grateful for their input which has significantly enhanced this final version.

Appendix

7.1   Data for the Standard Model

For each case of simple tension, the stress-free boundary condition determines the relation between the axial stretch and one of the other principal stretches, with the third stretch determined from the incompressibility condition. In each case, the axial stretch was specified and the other stretch as given in $(3.8)_2$, $(3.8)_4$ and $(3.8)_6$ was determined using the FindRoot function in Mathematica 10 (version number 10.0.1.0), with the AccuracyGoal option set equal to 3. The remaining principal stretch was determined from the incompressibility condition. The Cauchy stresses were determined from $(3.8)_1$, $(3.8)_3$ and $(3.8)_5$. The data used to construct the plot summaries of Section 4 are given below:

λ_x	λ_y	λ_z	σ_{xx} (kPa)
1	1	1	0
1.1	0.946	0.961	0.341
1.2	0.897	0.929	0.725
1.3	0.853	0.902	1.161
1.4	0.812	0.880	1.674
1.5	0.774	0.861	2.2644
1.6	0.741	0.844	2.935
1.7	0.709	0.830	3.726
1.8	0.679	0.818	4.645
1.9	0.652	0.807	5.682
2	0.627	0.798	6.897

λ_x	λ_y	λ_z	σ_{yy} (kPa)
1	1	1	0
0.950	1.1	0.957	0.307
0.903	1.2	0.923	0.634
0.860	1.3	0.894	0.985
0.821	1.4	0.870	1.373
0.785	1.5	0.849	1.797
0.751	1.6	0.832	2.276
0.719	1.7	0.818	2.819
0.690	1.8	0.805	3.415
0.662	1.9	0.795	4.102
0.637	2	0.785	4.845

λ_x	λ_y	λ_z	σ_{zz} (kPa)
1	1	1	0
0.957	0.950	1.1	0.338
0.92	0.906	1.2	0.675
0.887	0.867	1.3	1.009
0.857	0.833	1.4	1.345
0.831	0.802	1.5	1.696
0.806	0.775	1.6	2.049
0.784	0.750	1.7	2.421
0.764	0.727	1.8	2.808
0.745	0.706	1.9	3.207
0.728	0.687	2	3.626

Table 1: Simple tension data for the Standard Model (4.1) with $\gamma = 1$.

λ_x	λ_y	λ_z	σ_{xx} (kPa)
1	1	1	0
1.1	0.909	1.000	0.571
1.2	0.823	1.013	1.470
1.3	0.745	1.032	2.826
1.4	0.678	1.053	4.776
1.5	0.621	1.073	7.434
1.6	0.572	1.092	10.967
1.7	0.531	1.108	15.436
1.8	0.495	1.122	21.008
1.9	0.464	1.135	27.911
2	0.436	1.146	36.201

λ_x	λ_y	λ_z	σ_{yy} (kPa)
1	1	1	0
0.935	1.1	0.972	0.333
0.868	1.2	0.960	0.745
0.801	1.3	0.960	1.286
0.736	1.4	0.971	2.042
0.674	1.5	0.989	3.098
0.619	1.6	1.010	4.539
0.571	1.7	1.031	6.437
0.529	1.8	1.051	8.873
0.492	1.9	1.069	11.908
0.460	2	1.086	15.674

λ_x	λ_y	λ_z	σ_{zz} (kPa)
1	1	1	0
1.001	0.908	1.1	0.629
1.022	0.815	1.2	1.083
1.048	0.7349	1.3	1.446
1.071	0.667	1.4	1.779
1.088	0.613	1.5	2.107
1.102	0.567	1.6	2.443
1.114	0.528	1.7	2.792
1.123	0.495	1.8	3.156
1.130	0.466	1.9	3.537
1.137	0.440	2	3.936

Table 2: Simple tension data for the Standard Model (4.1) with $\gamma = 10$.

7.2 Data for the HGO model

For the HGO model (5.1), (5.4), the same procedure as described earlier was followed: the axial stretch was assumed prescribed and one of the remaining principal stretches determined from the stress-free boundary conditions. The remaining principal stretch was determined from the incompressibility condition and the axial stress then determined from the appropriate stress-stretch relation. The following data are summarized in the plots of Section 5.1:

λ_x	λ_y	λ_z	σ_{xx} (kPa)
1.000	1.000	1.000	0.000
1.100	0.931	0.976	0.643
1.200	0.869	0.959	1.542
1.300	0.808	0.952	2.919
1.400	0.746	0.958	5.194
1.500	0.679	0.982	9.285
1.600	0.604	1.034	17.541
1.700	0.521	1.129	36.374
1.800	0.432	1.287	84.774
1.900	0.341	1.543	229.903
2.000	0.256	1.952	743.198

λ_x	λ_y	λ_z	σ_{yy} (kPa)
1.000	1.000	1.000	0.000
0.960	1.100	0.947	0.303
0.921	1.200	0.905	0.606
0.881	1.300	0.873	0.918
0.843	1.400	0.847	1.248
0.805	1.500	0.828	1.604
0.768	1.600	0.814	1.995
0.731	1.700	0.805	2.432
0.695	1.800	0.799	2.921
0.661	1.900	0.796	3.475
0.627	2.000	0.797	4.119

λ_x	λ_y	λ_z	σ_{zz} (kPa)
1.000	1.000	1.000	0.000
0.981	0.927	1.100	0.390
0.966	0.863	1.200	0.757
0.955	0.805	1.300	1.115
0.946	0.755	1.400	1.469
0.939	0.710	1.500	1.826
0.933	0.670	1.600	2.191
0.929	0.633	1.700	2.566
0.925	0.601	1.800	2.953
0.922	0.571	1.900	3.354
0.920	0.543	2.000	3.771

Table 3: Simple tension data for the HGO model.

7.3 Data for Section 5.2

Exactly the same procedures as already described were applied in Section 5.2 for the HGO model (5.1), (5.5). The data used for the simple tension plots are the following:

λ_x	λ_y	λ_z	σ_{xx} (kPa)	λ_z	σ_{zz} (kPa)
1	1.0000	1.0000	0.0000	1.0	0.0000
1.1	0.9114	0.9975	0.4544	1.1	1.1087
1.2	0.8193	1.0171	1.1848	1.2	1.9802
1.3	0.7296	1.0543	2.4175	1.3	2.7035
1.4	0.6482	1.1020	4.4502	1.4	3.3305
1.5	0.5778	1.1538	7.6408	1.5	3.8941
1.6	0.5172	1.2084	12.5152	1.6	4.4158
1.7	0.4641	1.2675	19.9488	1.7	4.9106
1.8	0.4162	1.3348	31.5449	1.8	5.3891
1.9	0.3720	1.4148	50.2172	1.9	5.8590
2	0.3302	1.5142	81.8256	2.0	6.3263

Table 4: Simple tension data for the in-plane and out-of-plane modes of the HGO model (5.1), (5.5).

7.4 Data for Section 5.3

The data used in Figures 8 and 9 are given below:

axial stretch	σ_{xx} (kPa)	σ_{yy} (kPa)	σ_{zz} (kPa)	λ_x	λ_y	λ_z
1	0	0	0	1.0	1.0	1.0
1.1	9.055	8.203	46.04	1.1	0.9	1.0
1.2	27.29	23.74	83.37	1.2	0.8	1.1
1.3	68.38	57.63	115.9	1.3	0.7	1.2
1.4	157.0	131.0	140.8	1.4	0.6	1.3
1.5	333.9	277.5	163.8	1.5	0.5	1.4
1.6	693.3	567.2	190.6	1.6	0.4	1.6
1.7	1502	1189	212.3	1.7	0.3	1.8
1.8	3602	2707	253.8	1.8	0.3	2.1
1.9	10070	7042	276.5	1.9	0.2	2.6
2	34380	21920	338.1	2.0	0.2	3.3

Table 5: Simple tension data, to four significant digits where appropriate, for the HGO model (5.1), (5.6), together with the stretch data for simple tension in the x-direction.

References

Rivlin, R.S., 1948. Large elastic deformations of isotropic materials. I. Fundamental concepts. Philosophical Transactions of the Royal Society of London. Series A, Mathematical and Physical Sciences, 240, 459-490.

Holzapfel G.A., Gasser T.C., Ogden R.W., 2000. A new constitutive framework for ar-

terial wall mechanics and a comparative study of material models, J. Elasticity 61: 1-48

Murphy, J. G., 2014. Evolution of anisotropy in soft tissue. Proceedings of the Royal Society A: Mathematical, Physical and Engineering Science, 470, 20130548.

Horgan, C.O., Murphy, J.G., 2014. Some unexpected behaviour in shear for elasticity models of arterial tissue that only use the I_1, I_4, I_6 invariants. IMA Journal of Applied Mathematics, 79, 820-829.

Hosten, B., 1992. Stiffness matrix invariants to validate the characterization of composite materials with ultrasonic methods. Ultrasonics, 30, 365-371.

Kelly, A., Hine, P.J., Landert, M., Ward, I.M., 2005. The effect of the measurement frequency on the elastic anisotropy of fibre laminates. Journal of materials science, 40, 4461-4467.

Goriely, A. Tabor, M., 2013. Rotation, inversion and perversion in anisotropic elastic cylindrical tubes and membranes. Proceedings of the Royal Society of London A, 469, 20130011.

Holzapfel, G.A., Gasser, T.C. Ogden, R.W., 2004. Comparison of a multi-layer structural model for arterial walls with a Fung-type model, and issues of material stability. Journal of biomechanical engineering, 126(2), pp.264-275.

Holzapfel, G.A., Ogden, R.W., 2015. On the tension-compression switch in soft fibrous solids European Journal of Mechanics A/Solids 49 561-569.

Spencer, A.J.M ,1984. Constitutive theory for strongly anisotropic solids. In *Continuum Theory of the Mechanics of Fibre-reinforced Composites (Ed. A.J.M. Spencer). CISM Courses and Lectures No. 282*. Vienna: Springer Verlag.

Destrade, M., Martin, P.A. and Ting, T.C., 2002. The incompressible limit in linear anisotropic elasticity, with applications to surface waves and elastostatics. Journal of the Mechanics and Physics of Solids, 50, 1453-1468.

Shariff, M.H.B.M., 2011. Physical invariants for nonlinear orthotropic solids. International Journal of Solids and Structures, 48 1906-1914.

Shariff, M.H.B.M. and Bustamante, R., 2015. On the independence of strain invariants of two preferred direction nonlinear elasticity. Int. Jou. Engng. Science, 97, 18-25.

Fung, Y.C., Fronek, K. and Patitucci, P., 1979. Pseudoelasticity of arteries and the choice of its mathematical expression. American Journal of Physiology-Heart and Circulatory Physiology, 237(5), pp.H620-H631.

Chuong, C.J., Fung, Y.C., 1983. Three-dimensional stress distribution in arteries. Journal of biomechanical engineering, 105(3), pp.268-274.

Gültekin, O., Dal, H. and Holzapfel, G.A., 2016. A phase-field approach to model fracture of arterial walls: Theory and finite element analysis. Computer Methods in Applied Mechanics and Engineering in press.

Horgan, C.O., Murphy, J.G., 2016. The counterintuitive out-of-plane strength of incompressible orthotropic hyperelastic materials, submitted.

Shariff, M.H.B.M., 2016. Anisotropic separable free energy functions for elastic and non-elastic solids. Acta Mechanica, pp.1-25.